PEER-REVIEWED ARTICLE

Determining Coniferous Forest Cover and Forest Fragmentation with NOAA-9 Advanced Very High Resolution Radiometer Data

William J. Ripple

Abstract

NOAA-9 satellite data from the Advanced Very High Resolution Radiometer (AVHRR) were used in conjunction with Landsat Multispectral Scanner (MSS) data to determine the proportion of closed canopy conifer forest cover in the Cascade Range of Oregon. A closed canopy conifer map, as determined from the MSS, was registered with AVHRR pixels. Regression was used to relate closed canopy conifer forest cover to AVHRR spectral data. A two-variable (band) regression model accounted for more variance in conifer cover than the Normalized Difference Vegetation Index (NDVI). The spectral signatures of various conifer successional stages were also examined. A map of Oregon was produced showing the proportion of closed canopy conifer cover for each AVHRR pixel. The AVHRR was responsive to both the percentage of closed canopy conifer cover and the successional stage in these temperate coniferous forests in this experiment.

Introduction

On 7 October 1989 the United States Congress approved legislation requiring that federal agencies preserve contiguous stands of old-growth forests in the Pacific Northwest rather than harvest in a patchwork pattern resulting in forest fragmentation (Lehmkuhl and Ruggiero, 1991; Lord and Norton, 1990). This legislation was intended to protect the habitat of the northern spotted owl which needs large stands of old-growth forest to survive extinction (Ripple *et al.*, 1991b). With this legislation in place, developing methods for measuring the extent of forest cover and fragmentation at the landscape and regional level is important. Forest fragmentation has been documented at the landscape scale using a geographic information system to describe patch size, shape, abundance, spacing, and forest matrix characteristics (Ripple *et al.*, 1991a). Spatial data on forest fragmentation at a regional scale is typically not available.

The main objective of the research reported here was to describe the relationship between the proportion of coniferous closed canopy forest cover and AVHRR pixel radiance values. A second objective was to obtain spectral signatures from various forest successional stages using AVHRR data. With a ground resolution of approximately 1.1 km, AVHRR data can not detect individual disturbances such as clearcuts that average between 10 and 20 ha on public lands. However, it was hypothesized that radiance as measured by the AVHRR would have an inverse linear relationship with the proportion of coniferous closed canopy forest cover.

Apparently, few studies have been designed to determine cover of temperate coniferous forests with AVHRR data. Nelson (1989) attempted to use Global Area Coverage (GAC) AVHRR data with a 4-km resolution to estimate forest area for the entire United States. His results showed that GAC and MSS were not highly correlated. Loveland *et al.* (1991) included forests (coniferous and deciduous) in the development of their land-cover database for the conterminous United States. Their remote sensing estimates of forest cover were compared to other inventory approaches by Turner *et al.* (in press).

AVHRR satellite data have been used for regional estimates of forest cover in the tropical forests of South America and the eastern and southern hardwood forests of the United States. Nelson and Holben (1986) and Woodwell *et al.* (1987) used AVHRR data in conjunction with calibrations from the finer resolution Landsat Multispectral Scanner (MSS) data to discriminate cleared areas from primary forest in Brazil. Iverson *et al.* (1989) and Zhu and Evans (1992) used regression equations based on estimates of forest cover from Landsat Thematic Mapper (TM) data to determine the relationship between AVHRR data and forest cover. Townshend and Tucker (1984) found that AVHRR data represented 70 percent of MSS data variation during a land-cover mapping study. The normalized difference vegetation index (NDVI) [(near infrared − visible)/(near infrared + visible)] explained 70 percent and 79 percent of the variation in leaf area index in coniferous forest stands in western United States (Spanner *et al.*, 1990a). The authors concluded that reflectance was related to the proportion of surface cover types within AVHRR pixels as well as changes in leaf area index.

Study Area

The study area was in the western Cascade mountains of Oregon and encompassed both public USDA Forest Service land

Environmental Remote Sensing Applications Laboratory (ERSAL), Department of Forest Resources, Oregon State University, Corvallis, OR 97331.

Photogrammetric Engineering & Remote Sensing,
Vol. 60, No. 5, May 1994, pp. 533–540.

0099-1112/94/6001–533$03.00/0

on the Willamette National Forest and private land (Figure 1). The study area size was approximately 258,930 hectares, with elevations ranging from approximately 240 m to 1700 m above mean sea level. This area falls within portions of the western hemlock (*Tsuga heterophylla*) and Pacific silver fir (*Abies amabilis*) vegetation zones with the major tree species consisting of Douglas-fir (*Pseudotsuga menziesii*), western hemlock, Pacific silver fir, noble fir (*Abies procera*), and western red cedar (*Thuja plicata*) (Franklin and Dyrness, 1973). The topography is highly dissected by steep slopes with slope gradients ranging between approximately 0 and 60 degrees. The maritime climate has wet-mild winters and warm-dry summers. The landscape consists of large areas of old-growth Douglas-fir/western hemlock forests over 400 years old. Major disturbances include both fire and logging, resulting in a patchwork mosaic of herbaceous areas, deciduous shrubs and trees, and both natural and man-made closed canopy conifer forests. Areas of big leaf maple (*Acer macrophyllum*) and red alder (*Alnus rugosa*) are also found in the study area.

Methods

Part of a Landsat MSS scene acquired on 31 August 1988 was rectified using 7.5-minute orthophoto quadrangles. A nearest neighbor interpolation method was used to resample to a 50- by 50-m pixel size from the original 57- by 79-m pixel size. Using an unsupervised classified scheme, the delineated data were grouped into "closed canopy conifer forests" and "other areas" as part of a Landsat forest change project (Spies *et al.*, in press). The "closed canopy conifer forest cover" was old-growth, mature, and other conifer stands greater than approximately 30 to 40 years of age, and within-stand conifer canopy cover exceeded 60 percent (Brown, 1985). The term "closed canopy conifer forest cover" will be referred to as simply "closed conifer cover" in this paper. The "other areas" included clearcuts, young pre-canopy closure conifer plantations, shrubs, bare soil and rock, natural meadows, and water. Approximately 100 spectral classes were generated and were aggregated into the binary classification described above.

An accuracy assessment was conducted using a systematic sampling of 135 points across the study area. High-altitude, color-infrared photographs (scale 1:60,000) from July 1988 were used to check each of the 135 points. The cover at each point was identified on the aerial photography and compared to the category at the corresponding location on the classified image.

The AVHRR data were acquired in a local area coverage format from NOAA-9 orbit 18558 on the afternoon of 19 July 1988. A sub-scene of these data was rectified to UTM coordinates and registered to the MSS data set. AVHRR pixels were resampled to 1,000 by 1,000 m using a nearest-neighbor algorithm. The mean-square-error was 0.6 AVHRR pixels for the registration of the AVHRR data to the MSS data. Eighty-nine AVHRR pixels were selected systematically from the AVHRR set, and a window of 20- by 20-MSS pixels was selected to correspond to each AVHRR pixel. The visible (0.58 to 0.68 μm) and near infrared (NIR, 0.725 to 1.100 μm) band values were recorded for the 89 AVHRR pixels, and the percent closed conifer cover of each corresponding 20 by 20 MSS pixel window was computed. The percent closed conifer cover was defined as the proportion of an area or pixel containing closed conifer stands. Correlations were computed for the closed conifer cover, visible, and NIR variables along with the NIR/visible band ratio and the NDVI. In addition, the

Figure 1. Map showing the study area which was located on the west slopes of the Cascade Mountains in western Oregon.

AVHRR band values were converted to albedo using prelaunch calibration equations for the computation of a corrected band ratio and corrected NDVI (NOAA, 1991). Computing albedo from the AVHRR band values helps to allow for a direct comparison of NDVI values with other studies using AVHRR data (Spanner *et al.*, 1990b). A stepwise multiple regression was used to develop a model for predicting closed conifer cover from the AVHRR data. The model was validated by comparing predicted proportions of closed conifer cover for the entire study area to the proportion of closed conifer cover for the study area as determined from the MSS data set.

To determine spectral variation associated with successional changes, spectral signatures were extracted from this AVHRR data set for a set of homogeneous landscapes consisting of four different successional stages. These included a very large, disturbed clearcut area with an herbaceous/shrub canopy cover of approximately 90 percent (21 AVHRR pixels, 3 by 7); managed, closed-canopy Douglas fir forests approximately 40 years old with approximately 15 percent of the area in bigleaf maple and red alder (16 AVHRR pixels; 4 by 4); natural mature Douglas fir forests approximately 90 to 130 years old (21 AVHRR pixels, 3 by 7); and old-growth Douglas fir and western hemlock forests 400 to 600 years old (20 AVHRR pixels, 4 by 5). The mean AVHRR band values and standard deviations for each of these forest successional stages were plotted for the visible, NIR, and NDVI response.

Results

The MSS classification showed 57.8 percent of the study area in closed conifer cover with a total accuracy of 91 percent. A total of 74 out of 83 samples (89 percent) fell correctly into the closed conifer class, and a total of 49 out of 52 samples (94 percent) fell correctly into the "other land" category. The relationship between AVHRR pixel band values and closed conifer cover was inverse for both bands as expected (Figure 2). The visible ($r = -0.64$, $r^2 = 0.41$, $P<0.0001$) and NIR ($r = -0.63$, $r^2 = 0.40$, $P<0.0001$) bands showed much higher correlations with closed conifer cover than the albedo-corrected band ratio ($r = -0.14$, $r^2 = 0.02$, $P=0.190$) and the albedo-corrected NDVI ($r = -0.15$, $r^2 = 0.02$, $P=0.168$). The uncorrected band ratio ($r = -0.46$, $r^2 = 0.21$, $P<0.0001$) and the uncorrected NVDI ($r = -0.46$, $r^2 = 0.21$, $P<0.0001$) had significantly higher correlations with closed conifer cover than the albedo-corrected transformations (Figure 3).

Scatter diagrams between closed conifer cover and red or infrared AVHRR bands showed inverse linear relationships with random dispersal of points. The step-wise multiple

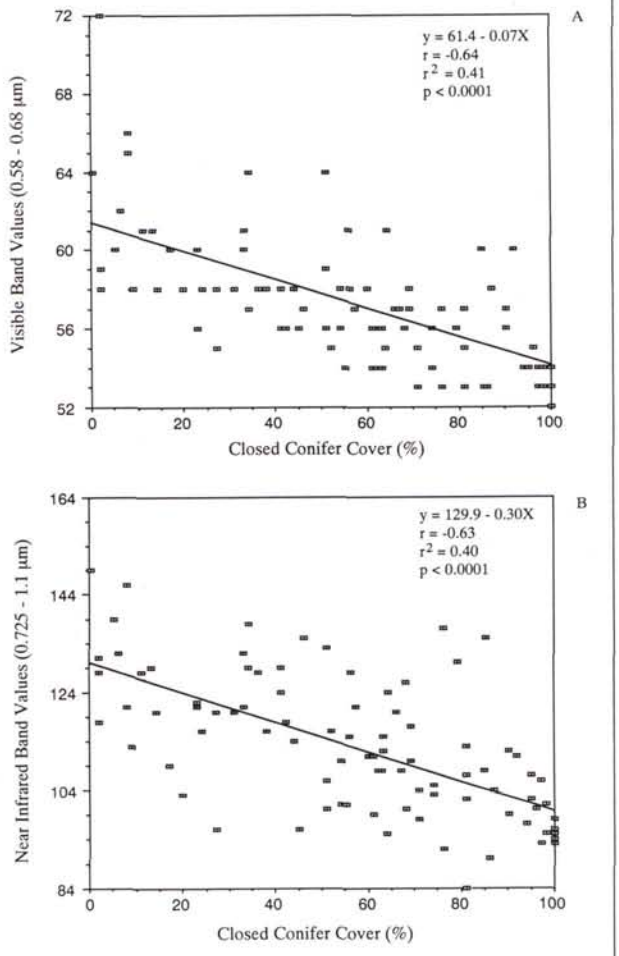

Figure 2. Scatter diagram and simple linear regression of (a) AVHRR visible band values and percent closed conifer cover along with simple linear regression of (b) AVHRR near infrared band values and percent closed conifer cover.

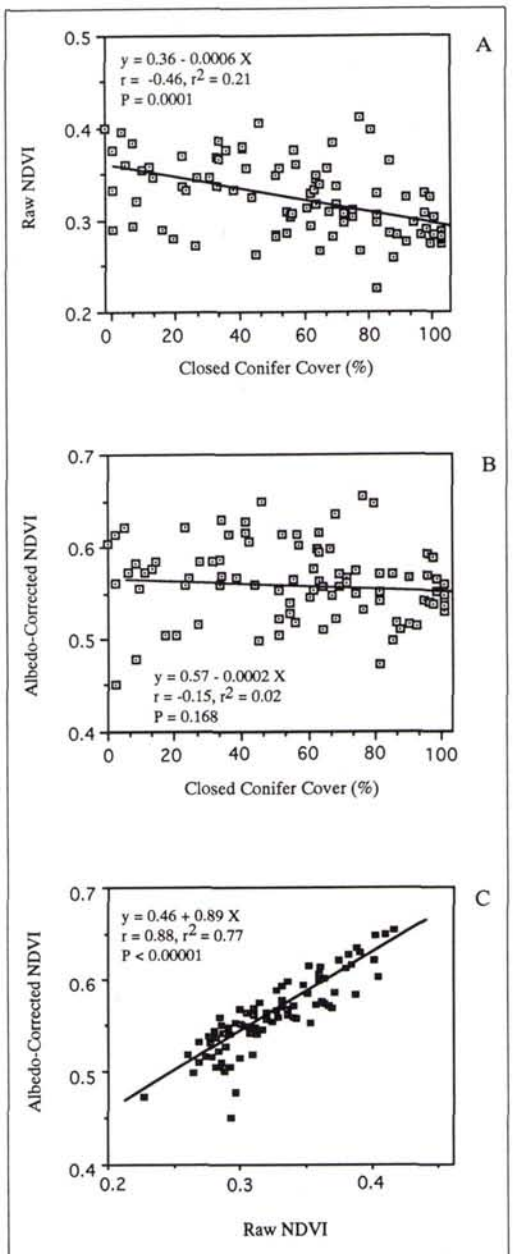

Figure 3. Scatter diagrams and simple linear regression of (a) raw NDVI and percent closed conifer cover, (b) albedo-corrected NDVI and percent closed conifer cover, and (c) albedo-corrected NDVI and raw NDVI.

regression resulted in the model: percent closed conifer cover = 335.53 − 3.42 (visible) − 0.73 (NIR) with an adjusted coefficient of determination of 0.46 ($P<0.001$). When the above model was applied to the entire study area of 2405 AVHRR pixels, the mean percentage of closed conifer cover was 54.7 percent which compared favorably with the original MSS estimate of 57.8 percent. Spatial patterns in the AVHRR data from the model output were similar to the MSS patterns (Figure 4).

Figure 5 shows AVHRR band values related to forest successional stage. Band values decreased with forest succession for both the visible and NIR bands. It should be noted that these decreases were after the establishment of herbs and shrubs on the landscape. The visible band showed the greatest difference between mean band values for herb/shrub and young closed canopy conifers. The NIR showed the greatest difference between mean band values between young conifer and mature forests as well as between mature and old-growth band values. The NDVI values were lowest for the herb/shrub class, highest for the young conifer class, and intermediate for mature and old-growth forests.

Discussion

The results from this experiment indicate that it may be possible to use AVHRR data to obtain landscape and regional estimates of closed conifer cover in the temperate coniferous forests. Bands 1 and 2 were related to both the proportion of

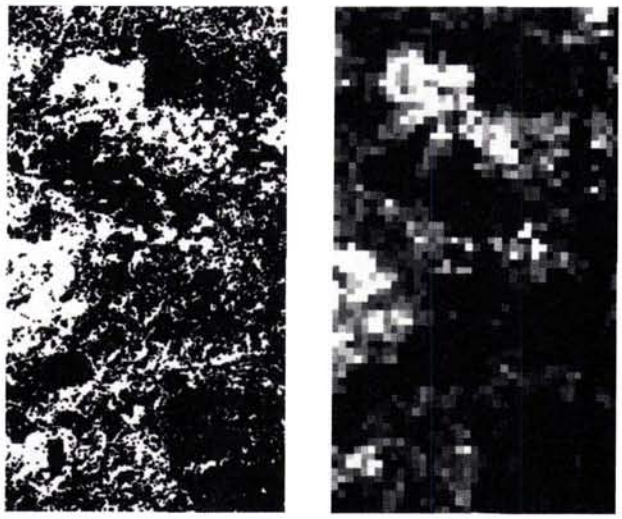

Figure 4. The image on the left shows closed conifer cover in black and other lands in white. It was produced from classified Landsat MSS data (50-m pixels). The right image is a gray scale of AVHRR data (1,000-m pixels) showing the percentage of closed conifer cover within AVHRR pixels (low percentages are light and high percentages are dark).

closed conifer cover within AVHRR pixels and the seral stage of the vegetation. Both visible and NIR band values decreased linearly with the proportion of closed conifer cover within a pixel. This result is in contrast to the typically found direct relationship between NIR and vegetation amount for many vegetation types. Researchers have found that this direct relationship between NIR with measures of conifer amount does not always exist, especially for canopies that are not closed. When the background or understory is brighter than the conifer canopy, the relationship can be inverse (Ripple *et al.*, 1991c), and when the background is darker or the canopy is closed, it can be direct (Spanner *et al.*, 1990a). When the background has about the same brightness as the conifers or is highly variable, the relationship to NIR may be flat or weak. It has also been hypothesized that conifer canopy shadowing contributes to an inverse NIR relationship as the canopy structure becomes more complex and shaded in older stands (Ripple *et al.*, 1991c). The reason for the inverse relationships between the band values and closed conifer cover in this study was attributed to the deciduous shrubs and trees along with herbaceous vegetation being more highly reflective than the conifer canopy in both the visible and NIR bands (Fiorella and Ripple, 1993). Areas within AVHRR pixels not covered by a conifer canopy consisted mostly of herbaceous or deciduous woody vegetation with very little bare soil. Therefore, band values decreased as the proportion of the darker conifer cover increased.

The NDVI relationship with closed conifer cover was also inverse, but the correlation was not as high as with the visible and NIR bands. The two-variable (band) regression model accounted for more variance than either the NDVI or the individual bands. These results are similar to those found by Iverson *et al.* (1989). The variance not accounted for in this regression model was attributed to slight misregistration between the AVHRR and MSS data sets and variability in the broad successional stages. The mean-square error of 0.6 AVHRR pixels, equivalent to approximately 600 metres on the ground, may have been the cause for some of the scatter around the regression lines. Overall, the model worked well, considering that each AVHRR pixel represented 400 times more land area than each Landsat MSS pixel.

It should be noted that the albedo-corrected NDVI and the uncorrected NDVI were not perfectly correlated ($r = 0.88$, $r^2 = 0.77$, Figure 3c). The albedo-corrected NDVI had a lower correlation to the percentage of closed conifer cover than the uncorrected NDVI. The differences between the uncorrected and corrected NDVI values were greater than the rounding errors inherent in the transform from the original AVHRR band values to the albedo-corrected NDVI. Most recent research on the calibration of AVHRR has been concerned with post-launch performance of the sensor, and specifically the degra-

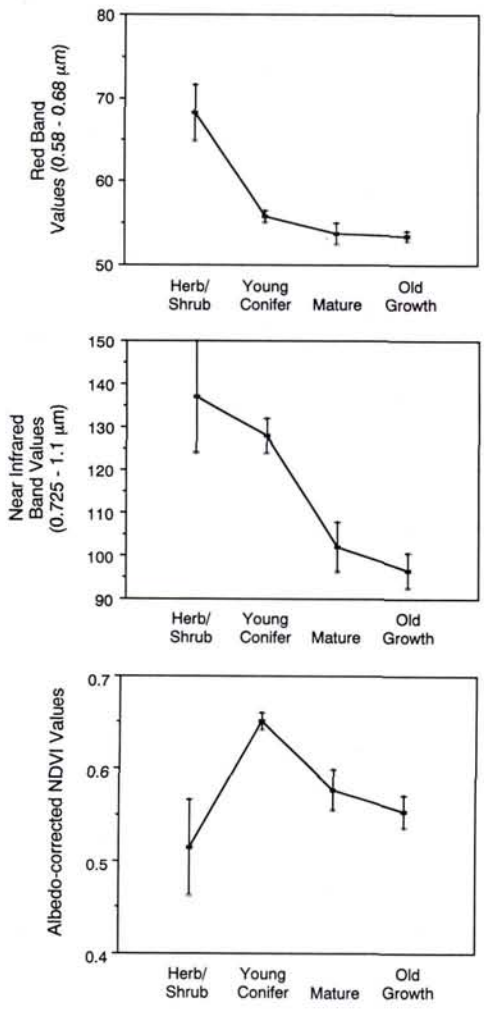

Figure 5. Band value means and standard deviations using the visible, near infrared, and the normalized differences vegetation index (NDVI) from AVHRR data for four successional stages found on the west slope of the Cascades of Oregon.

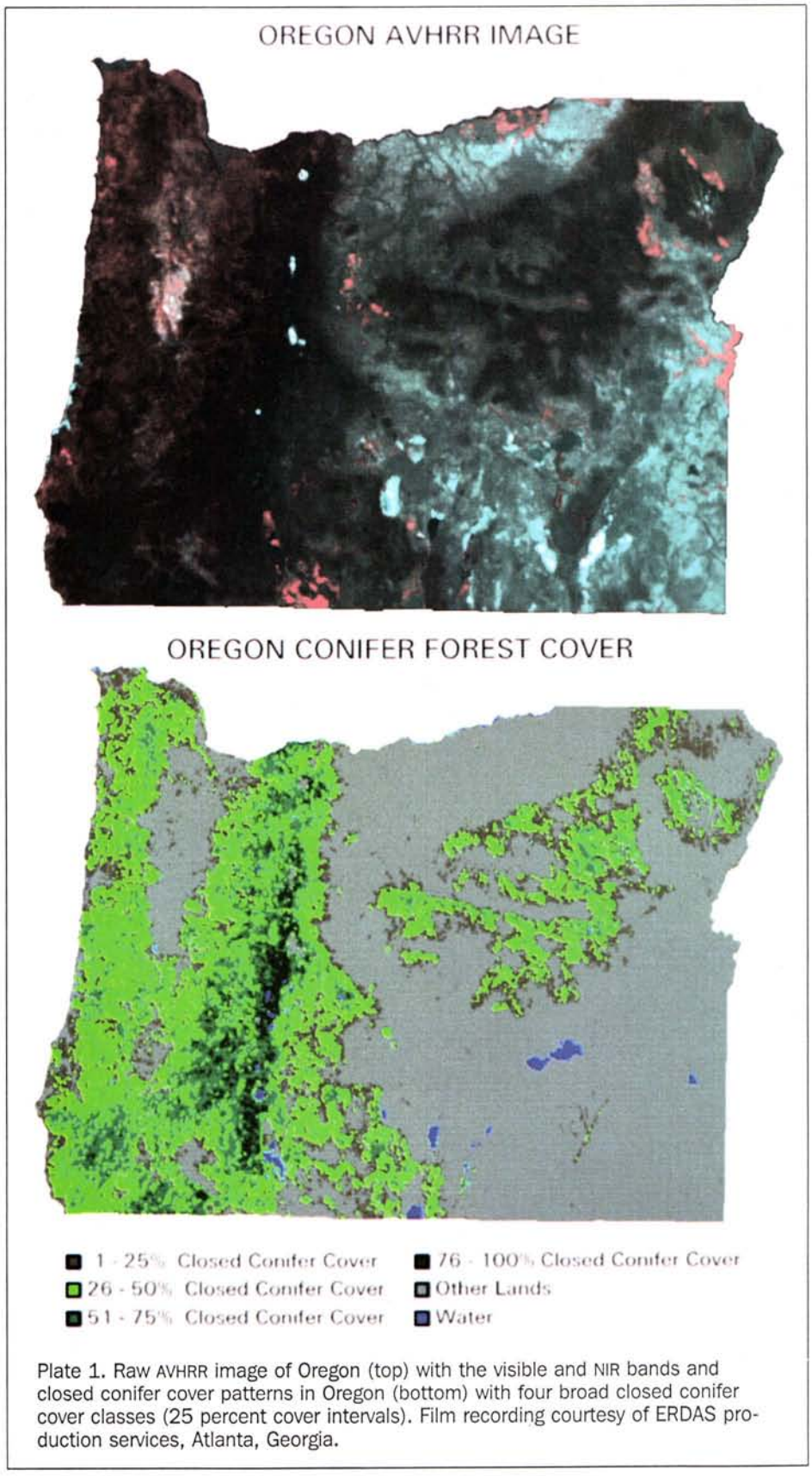

Plate 1. Raw AVHRR image of Oregon (top) with the visible and NIR bands and closed conifer cover patterns in Oregon (bottom) with four broad closed conifer cover classes (25 percent cover intervals). Film recording courtesy of ERDAS production services, Atlanta, Georgia.

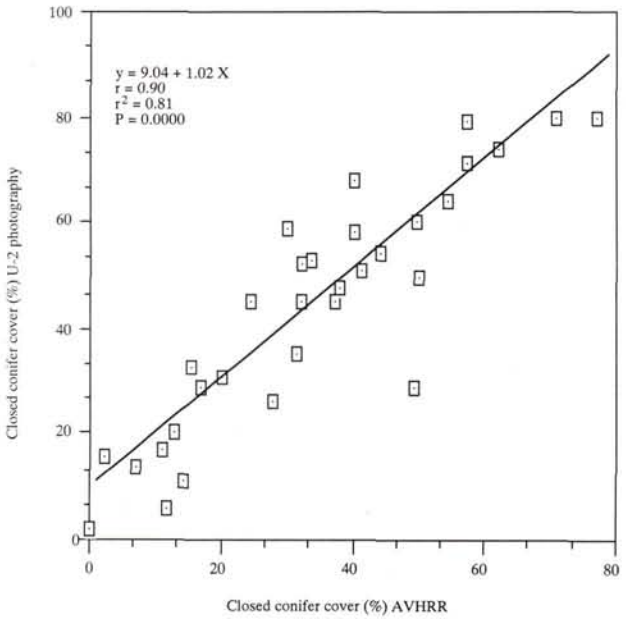

Figure 6. Comparison of estimates of closed conifer cover from AVHRR satellite data and from U-2 aerial photography for 32 7.5-minute quadrangles in Oregon.

dation in the instrument gain values over time because no on-board calibration is available (Che and Price, 1992; Kaufman and Holben, 1993). Because of this degeneration over time, it is especially important to use post-launch calibration procedures in studies comparing multiple AVHRR images. Off-nadir viewing, atmospheric variability, and instrument precision also creates errors in NDVI observations (Goward *et al.*, 1991). Little information is available on the effects transforming raw AVHRR values into calibrated values and then in turn converting those calibrated values into NDVI space. The discrepancy between raw NDVI and Albedo-corrected NDVI values apparently result from two different locations in cartesian space (NIR, red coordinates) being non-linearly transformed into polar (NDVI) space. Similar discrepancies could also exist in other situations where satellite band values are corrected before transforming them into a ratio like the NDVI.

The relationship between visible band values and forest successional stage was inverse and somewhat asymptotic after canopy closure. The largest mean differences between the seral stages of young and mature, and mature and old-growth were found using the NIR band. NIR band values between the seral stages of herb/shrub and closed canopy young conifer decreased because of decreased deciduous vegetation exposed to the sensor. This trend continued between the closed canopy young conifer and the mature conifer seral stage as the increase in canopy shadowing and decrease of the bright deciduous component apparently dominated off-setting increases in NIR due to increases in leaf area index (Ripple *et al.*, 1991c; Spanner *et al.*, 1990a). NIR values for old-growth were slightly lower than mature forest. This was probably due to the increase in shadowing and canopy gaps dominating the signal resulting in a lower radiance for old-growth (Fiorella and Ripple, 1993). This was not likely due to the higher leaf area index in the old-growth, because light becomes asymptotic above a LAI of 6 (Spanner *et al.*, 1990b) and old-growth LAIs are normally higher than 6 in this area (Franklin *et al.*, 1981).

NVDI increased from the herb/shrub stage to the young conifer stage and then decreased through the mature to the old-growth stage indicates a potential problem with using NDVI for successional stage mapping. Within these temperate coniferous forests, it appears that both pre-and post-canopy closure NDVI values could be confused. Spanner *et al.* (1989) had similar results when using the similar TM band 4/3 ratio in these forests. Box *et al.* (1989) also concluded that there did not seem to be any reliable relationship, across different vegetation structures, between biomass and NDVI when using AVHRR data. Multiple regression of individual bands may be the best approach for successional stage mapping with AVHRR.

Application of Results

The results presented above have applications in both measuring the total extent of coniferous forests and the level of forest fragmentation for larger regions. For example, the regression model was also applied to the entire state of Oregon to determine the spatial distribution of conifer forests and levels of forest fragmentation. The resulting state map showed closed conifer cover ranging from 0 to 100 percent in 1 percent increments just as in Figure 4 above for the small area. Because it was not feasible to show a map of all 100 classes for the entire state, a generalized map was produced showing the estimates of the proportion (in 25 percent steps) of closed conifer cover for each AVHRR pixel in the state (Plate 1). Within western Oregon, the map showed the highest levels of forest fragmentation in the Oregon Coast Range and the lowest fragmentation in the southern Cascade Mountains, especially in and around the Umpqua National Forest. The map can also be used to analyze landscape linkages for biodiversity planning and ecosystem management. For example, it showed the various levels of fragmentation on forest corridors linking the Cascade range with both the Coast Range and the Klamath Mountains.

The AVHRR-based Oregon map showed 10,891,000 ha of conifer forests in Oregon. This is 4 percent higher than estimated by the U.S. Forest Service under the Resources Planning Act (RPA). The RPA estimated 10,463,827 ha of conifer and 890,750 ha of hardwoods for a total of 11,354,577 ha of forest land in Oregon. The land-cover database for the conterminous United States shows total forest land in Oregon at 11,990,000 ha (Loveland *et al.*, 1991; Turner *et al.*, in press).

This state-wide data set of percentage of closed conifer cover was verified through a comparison with U-2 color-infrared aerial photography flown by NASA on 19 July 1988. The flight covered parts of the central Oregon Coast range, the north Cascade range, the central Cascade range, and the Blue Mountain range in northeastern Oregon. Eight 7.5-minute quadrangles were randomly selected in each of these four geographic areas to compare with the AVHRR set. The proportion of closed conifer cover in each of these 32 quadrangles was estimated using a dot grid on the U-2 photography. These same 32 quadrangles were windowed out of the AVHRR closed conifer cover data set.

The proportion of closed conifer cover as estimated from AVHRR was highly correlated ($r^2 = 0.81$) with estimates from the U-2 photography (Figure 6). The regression between these two sets showed a linear relationship with the U-2 photos providing slightly higher estimates of closed conifer cover

than the AVHRR set (intercept = 9.04). This difference was probably due to the ability to detect very small conifer patches on the U-2 photography.

The relationship between AVHRR pixel values with the proportion of closed conifer cover indicate that these sensor data may be well suited as an integrator for large area forest fragmentation studies in this Pacific Northwest region. For example, these AVHRR results were used in designing proposed federal legislation for locating biological forest reserves to protect the northern spotted owl and other important wildlife species (Forest Ecosystem Management Team, 1993).

Conclusions

This research has shown that band values in the AVHRR channels 1 and 2 are related to the continuum of forest landscape conditions. The regression model was successful because areas that were highly fragmented by clearcutting had high band values in both the visible and near infrared bands. Conversely, areas dominated by late-successional forests and low fragmentation consistently had the lowest band values.

Additional research should be conducted to confirm the spectral/successional stage relationships found here. This work could include research using pixel mixture models (Smith *et al.*, 1990) to develop a better understanding of how the proportions of successional stages and forest cover determine the spectral response in large AVHRR pixels. Caution should be used when making calibration corrections before calculating the NDVI and in attempting to use the NDVI when considering data sets that include both natural and managed stands with a range of structural characteristics and successional stages (i.e., herbs, deciduous shrubs, conifers, etc.). It appears that AVHRR has potential for estimating forest fragmentation in temperate coniferous forests and for mapping the spatial distribution of forest resources at continental and global scales.

Acknowledgments

This project was funded in part by NASA grant number NAGW - 1460. The author would like to thank G.A. Bradshaw, Louis Iverson, RJay Murray, Mike Spanner, Dave Turner, and Denis White for their helpful comments on an earlier version of the manuscript. Maria Fiorella and Jon Greninger assisted in various aspects of the mapping.

References

Box, E.O., B.N. Holben, and V. Kalb, 1989. Accuracy of AVHRR Vegetation Index as a Predictor of Biomass, Primary Productivity and Net CO_2 Flux, *Vegetation*, 80:71-89.

Brown, E.R. (editor), 1985. *Management of Wildlife and Fish Habitats in Forests of Western Oregon and Washington*, No. R6-FLWL-192-1985, Pacific Northwest Region, USDA Forest Service, Portland, Oregon.

Che, N., and J.C. Price, 1992. Survey of Radiometric Calibration Results and Methods for Visible and Near Infrared Channels of NOAA-7, -9, and -11 AVHRRs, *Remote Sensing of Environment*, 41:19-27.

Fiorella, M., and W.J. Ripple, 1993. Determining Successional State of Temperate Coniferous Forests with Landsat Satellite Data, *Photogrammetric Engineering & Remote Sensing*, 59(2):239-246.

Forest Ecosystem Management Assessment Team, 1993. *Forest Ecosystem Management: An Ecological, Economic, and Social Assessment*, USDA Forest Service, Portland, Oregon.

Franklin, J.F., and C.T. Dyrness, 1973. *Natural Vegetation of Oregon and Washington*, Oregon State University Press, 452 p.

Franklin, J.F., K. Cromack, Jr., W. Denison, A. McKee, C. Maser, J. Sedell, F. Swanson, and G. Juday, 1981. *Ecological Characteristics of Old-Growth Douglas-Fir Forests*, General Technical Report PNW-118, USDA Forest Service, Pacific Northwest Forest and Range Experiment Station, Portland, Oregon, 417 p.

Goward, S.N., B. Markham, D.G. Dye, W. Dulaney, and J. Yang, 1991. Normalized difference vegetation index measurements from the advanced very high resolution radiometer, *Remote Sensing of Environment*, 35:257-277.

Iverson, L.R., E.A. Cook, and R.L. Graham, 1989. A technique for extrapolating and validating forest cover across large regions calibrating AVHRR data with TM data, *International Journal of Remote Sensing*, 10(11):1805-1812.

Kaufman, Y.J., and B.N. Holben, 1993. Calibration of the AVHRR Visible and Near-IR Bands by Atmospheric Scattering, Ocean Glint, and Desert Reflection, *International Journal of Remote Sensing*, 14(1):21-52.

Lehmkuhl, J.F., and L.F. Ruggiero, 1991. Forest fragmentation in the pacific northwest and its potential effects on wildlife, *Wildlife and Vegetation of Unmanaged Douglas-fir forests*, General Technical Report PNW-GTR-285, USDA Forest Service, Pacific Northwest Research Station, Portland, Oregon, pp. 35-46.

Loveland, T.R., J.W. Merchant, D.O. Ohlen, and J.F. Brown, 1991. Development of a land-cover characteristics database for the conterminous U.S., *Photogrammatic Engineering & Remote Sensing*, 57(11):1453-1463.

Lord, J.M., and D.A. Norton, 1990. Scale and the spatial concept of fragmentation, *Conservation Biology*, 4(2):197-202.

Nelson, R., 1989. Regression and ratio estimators to integrate AVHRR and MSS data, *Remote Sensing of Environment*, 30:210-216.

Nelson, R., and B. Holben, 1986. Identifying deforestation in Brazil using multiresolution satellite data, *International Journal of Remote Sensing*, 7(3):429-448.

NOAA, 1991. *Polar Orbiter Data Users Guide*, National Oceanic and Atmospheric Administration, National Environmental Satellite, Data, and Information Service, National Climatic Data Center, Satellite Data Services Division, Washington, D.C.

Ripple, W.J., G.A. Bradshaw, and T.A. Spies, 1991a. Measuring forest landscape patterns in the Cascade Range of Oregon, USA, *Biological Conservation*, 57:73-88.

Ripple, W.J., D.H. Johnson, K.T. Hershey, and E.C. Meslow, 1991b. Old-Growth and Mature Forests Near Spotted Owl Nests in Western Oregon, *Journal of Wildlife Management*, 55(2):316-318.

Ripple, W.J., S. Wang, D.L. Isaacson, and D.P. Paine, 1991c. A preliminary comparison of Thematic Mapper and SPOT-1 HRV multispectral data for estimating coniferous forest volume, *International Journal of Remote Sensing*, 12(9):1971-1977.

Smith, M.O., S.L. Ustin, J.B. Adams, and A.R. Gillespie, 1990. Vegetation in deserts: I. A regional measure of abundance from multispectral images, *Remote Sensing of Environment*, 31:1-26.

Spanner, M.A., C.A. Hlauka, and L.L. Pierce, 1989. Analysis of forest disturbance using TM and AVHRR Data, *Proceedings of International Geoscience and Remote Sensing Symposium*, Vancouver, Canada, 10 July, pp. 1387-1390.

Spanner, M.A., L.L. Pierce, D.L. Peterson, and S.W. Running, 1990a. Remote sensing of temperate coniferous forest leaf area index: The influence of canopy closure, understory vegetation and background reflectance, *International Journal of Remote Sensing*, 11(1):95-111.

Spanner, M.A., L.L. Pierce, S.W. Running, and D.L. Peterson, 1990b. The seasonality of AVHRR data of temperate coniferous forests: Relationship with leaf area index, *Remote Sensing of Environment*, 33:112.

Spies, T.A., W.J. Ripple, and G.A. Bradshaw, in press. Dynamics and pattern of a managed coniferous forest landscape, *Ecological Applications*.

Townshend, J.R.G., and C.J. Tucker, 1984. Objective assessment of Advanced Very High Resolution Radiometer data for land cover mapping, *International Journal of Remote Sensing*, 5(2):497-504.

Turner, D.P., G. Koerper, H. Gucinski, and C. Peterson, 1993. Monitoring global change: Comparison of forest cover estimates using remote sensing and inventory approaches, *Environmental Monitoring and Assessment*, 26:295-305.

Woodwell, G.M., R.A. Houghton, T.A. Stone, R.F. Nelson, and W. Kovalick, 1987. Deforestation in the tropics: New measurements in the Amazon Basin using Landsat and NOAA AVHRR imagery, *J. Geophys. Res.*, 92(02):2157-2163.

Zhu, Z., and D.L. Evans, 1992. Mapping midsouth forest distributions, *Journal of Forestry*, 90(12):27-30.

(Received 19 February 1993; revised and accepted 10 August 1993)